Status of Ion Engine Development for High Power, High Specific Impulse Missions*†

Vincent K. Rawlin
National Aeronautics and Space Administration
Glenn Research Center MS 301-3
21000 Brookpark Rd
Cleveland, OH 44135
216-977-7462
Vince.Rawlin@grc.nasa.gov

George J. Williams
Ohio Aerospace Institute
NASA Glenn Group MS 301-3
21000 Brookpark Rd
Cleveland, OH 44135
216-433-9622
George.J.Williams@lerc.nasa.gov

Luis R. Piñero
National Aeronautics and Space Administration
Glenn Research Center MS 301-3
21000 Brookpark Rd
Cleveland, OH 44135
216-977-7428
Luis.R.Pinero@grc.nasa.gov

Robert F. Roman
QSS Group, Inc.
Glenn Research Center MS 16-1
21000 Brookpark Rd
Cleveland, OH 44135
216-433-2055
Robert.F.Roman@grc.nasa.gov

IEPC-01-096

A high-voltage ion optics design was chosen for an assumed mission that required a long-life, high power, high specific impulse krypton ion engine. Such an engine could support energetic space missions to the outer planets or beyond. Detailed performance and lifetime analyses and several inexpensive sub-scale grid tests were conducted. A sub-scale grid set of the selected geometry was tested at voltages up to 13,000 volts and yielded a krypton ion beam current that, when scaled to a full-size 50-cm diameter, would produce an ion beam with a power of 30 kW at a specific impulse over 14,000 seconds. The operational ion beam focusing limits, as a function of ion current per hole, were found to impose requirements of high uniformity on the discharge chamber plasma density. Fabrication of full-size, two-grid, 50-cm diameter titanium ion optics has begun.

Introduction

NASA is contemplating the exploration of outer planets and interstellar space.[1-4] One of the advanced propulsion technologies under consideration for near-term missions is Nuclear Electric Propulsion (NEP). Ion engines, similar to the successful NASA Solar Electric Propulsion Technology Applications Readiness (NSTAR) thruster[5] that is currently being flown on Deep Space One,[6] would provide the propulsion. The NSTAR thruster has full-power ratings of 2.3 kW at a specific impulse of 3100 seconds with 12000 hours life and may be power-throttled to 500 Watts. NEP systems for energetic outer planet and interstellar space missions will certainly require multiple, higher-powered (>10 kW) thrusters operating at much greater values of specific impulse (>8000 seconds), for significantly longer times (>3 years), and probably at a fixed operating point.

The power consumed in an efficient gridded ion thruster can be approximated as the product of the beam current and the sum of the beam voltage and discharge losses (expressed as watts per ampere of beam current). Currently, typical values of primary propulsion ion thruster beam current and discharge losses are a few amperes and 150-350 W/A,

* Presented as Paper IEPC-01-096 at the 27th International Electric Propulsion Conference, Pasadena, CA, 15-19 October 2001.

respectively, depending on the propellant type and input power level. The area of the ion extraction system grows with beam current due to both space charge limitations of the ion thruster grids and lifetime considerations at large values of beam or discharge ion current densities. Therefore, a practical way of increasing both thruster power and specific impulse is to raise the beam voltage.

The development of early laboratory ion thrusters in the United States was conducted assuming the availability of high power, lightweight space nuclear power sources. Thus, the optimum values of specific impulse for missions of interest were in the 8-10,000 second range with mercury as the propellant.[7,8] As ion thruster technology evolved in the 1960's[9] and solar arrays were developed for space propulsion applications, the anticipated specific impulse for flight decreased to about 4000 seconds, as demonstrated in space on Space Electric Rocket Tests (SERT) I and II.[10,11] During space mission planning at JPL[12] in the early 1970's, the optimum specific impulse for primary propulsion with 30-cm diameter mercury ion thrusters had decreased to 3000 seconds. With the development of the Solar Electric Propulsion System (SEPS)[13] and the Ion Auxiliary Propulsion System (IAPS)[14] over the next decade, mercury ion propulsion matured. In the early 1980's, the propellant of choice was switched from mercury to xenon.[15,16] Further ion thruster development[17] and technology transfer has led to operational flights of Xenon Ion Propulsion Systems (XIPS) for auxiliary propulsion[18,19] with specific impulse values of 2600 or 3800 seconds and primary propulsion[5] at 3100 seconds.

A multi-phase program at NASA's Glenn Research Center was initiated last year to develop a 10-30 kW, krypton ion engine capable of operating at values of specific impulse in excess of 10,000 seconds and for up to 10 years. In the first phase, a 76-cm diameter discharge chamber was designed and fabricated to allow increased ion extraction area as a means of increasing thruster power at low and high specific impulse.[20] Reference 20 reported initial test results in which the discharge chamber performance was evaluated with xenon and krypton propellants. An ion beam was accelerated, with a novel ion extraction system consisting of three sets of NSTAR grids, to a specific impulse of 3800 seconds, but only with xenon.

The second phase of the program has concentrated on the development of ion optics that would allow krypton ion thruster operation up to 30 kW at high specific impulse based on assumed requirements for an Interstellar Precursor Mission. The thruster-relevant mission requirements assumed krypton propellant, a specific impulse of 14,000 seconds, a thruster power of 30 kW, and a thruster life of 10 years. These translated into ion optics requirements of a net accelerating voltage of 13,000 volts, a 2.3 ampere beam current, thicker (than NSTAR) grids, lower beam current densities, and a flatter discharge plasma density profile.

An ion optics design effort based on cost, performance, and lifetime considerations was conducted. A 2-D computer code and prior ion optics studies[21-23] were used to determine preliminary designs. Concurrently, several sub-scale sets of ion extraction grids were fabricated and tested at values of beam current density and exhaust velocity expected for 30 kW operation. Based on the results of sub-scale grid tests, full-scale grids have been designed, materials have been purchased, and their fabrication has begun.

The latest results of this high power, high specific impulse thruster development program are presented.

Apparatus

Computer Model

A 2-dimensional computer code was used at GRC to simulate the ion flow in 2-grid optics proposed for high specific impulse operation. The code, named OPT, was developed by Ishihara and Arakawa at the University of Tokyo, Japan and modified at Colorado State University by Nakayama.[24]

Thruster

The basis for the design of high power, high specific impulse ion optics was the 76-cm diameter thruster,[20] shown in Figure 1, which was developed for NASA's Code S Cross-Cutting Technology Enterprise Program.

Figure 1 - High-power, 76-cm diameter ion thruster.

The upstream end employs a single, on-axis, NSTAR engineering model cathode. There are 9 rings of high field strength, rare-earth permanent magnets with alternating polarity along the back-plate and cylindrical section. The extraction grid plate shown was used to mount 3 sets of NSTAR ion optics for the prior effort. One of these openings was used for sub-scale grid tests presented herein while the other two openings were sealed, as shown in Figure 2. Another grid plate was fabricated to accept a set of 50-cm optics for plasma density profile measurements and future full-size optics.

An additional modification for tests at high voltage was to remove the low-voltage NSTAR propellant isolators and replace them with long lengths of fluoroelastomer tubing to serve as low-pressure, high-voltage isolation between the thruster and the grounded feed system. In separate bell-jar tests this scheme appeared adequate, but, when used with the thruster at voltages beyond 10 kV, there were frequent over-current conditions.

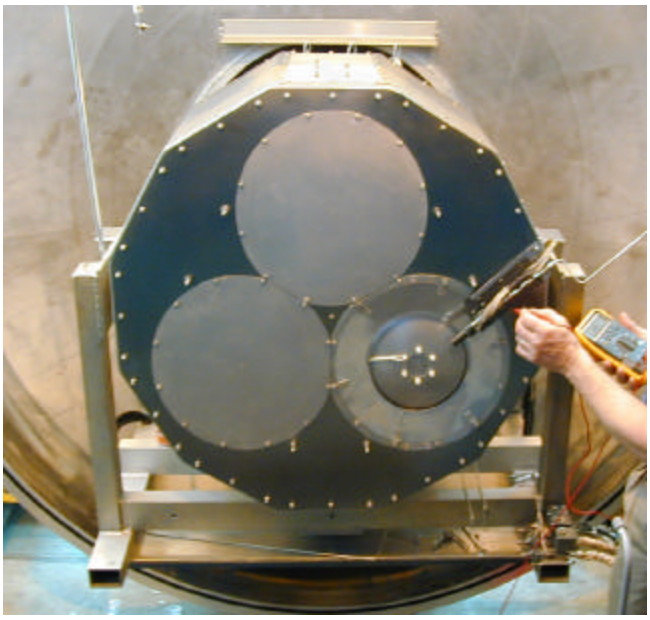

Figure 2 - Thruster with sub-scale grid set 2.

An engineering model NSTAR neutralizer was used for tests with sub-scale grids. It was mounted at either the top of the thruster, as shown in Figure 1, or close to the sub-scale grids as, shown in Figure 2.

Sub-scale Ion Accelerating Grids

Three sub-scale sets of 19-hole, 2-grid ion optics were fabricated and tested, one set at a time, on the high-power discharge chamber to evaluate different electrode geometries at high specific impulse conditions. The properties of each set of electrodes are given in Table 1. The thickness of each grid was based on initial estimated lifetime requirements for stainless steel grids. The screen grids were 2.9-mm thick stainless steel and accelerator grids were 3.7-mm thick molybdenum, although 4-mm thick stainless steel was desired. These sub-scale flat electrodes were each mounted to domed stainless steel disks from which the centers had been removed. The screen and accelerator grids were each electrically isolated from their stainless steel domed disks to allow independent measurements of current striking each grid and domed disk. The domed stainless steel disks were each mounted to a molybdenum stiffening-ring. Each pair of stiffening rings was separated with 6 insulators to give the desired cold grid spacing. Based on the beam profile results of reference 20, it was assumed that the sub-scale grids were located where the plasma density was fairly uniform throughout the perforated area.

Table 1. Electrode Set Dimensions

Parameter	Sub-scale set 1 (Scaled NSTAR design)	Sub-scale set 2	Sub-scale set 3
Beam diameter, cm	11.2	4.7	4.7
Number of holes	19	19	19
Center-to-center hole spacing, mm	23.0	9.5	9.5
Screen grid hole diameter, mm	19.6	8.84	8.84
Screen grid open area fraction	0.66	0.79	0.79
Screen grid thickness, mm	2.92	2.92	2.92
Accelerator grid hole diameter, mm	12.3	3.99	5.00
Accelerator grid open area fraction	0.26	0.16	0.25
Accelerator grid thickness, mm	3.71	3.71	3.71
Grid-to-grid spacing, mm	6.5	9.0	9.0

Facilities

All high-power ion thruster testing was conducted in NASA GRC's Vacuum Facility 11 (VF11). VF11 is 2.2-m in diameter by 9.0-m in length. Four 0.9-m diameter and three 1.2-m diameter helium cryopumps yield a pumping speed of approximately 240,000 liters per second (nitrogen). A 2-D motion control system was used to move a Faraday probe radially and axially through the plasma plume.[25] Resident optical diagnostics include CCD cameras for observation. Krypton was provided to the thruster through calibrated flowmeters. For all tests with sub-scale grids, the facility pressure never exceeded 1.3 $x10^{-4}$ Pa.

Power Supplies

The high-power console, used for tests reported herein, was an assembly of commercial power supplies similar to the power console described in reference 26. Major differences between these power consoles follows. The high-power console used a 30 kV, 0.2 A power supply, with a grounded negative output, for all sub-scale grid tests. Two accelerator power supplies were used. A 3 kV, 7 mA power supply was used for testing sub-scale grid set 1, while a 600 V 1.6 A power supply was used for grid sets 2 and 3. The discharge power supply provided up to 40 A. The ON/OFF and output controls for the discharge and cathode heater power supplies were isolated by analog fiber-optic links. The output controls for the beam, accelerator, neutralizer keeper, and neutralizer heater power supplies were isolated using individual control power supplies.

Procedure

Analyses

A number of different grid geometries and operating conditions were evaluated with the OPT code to provide a starting point for the grid designs in a manner similar to that described in reference 27. Cases were run to determine approximate values of beamlet divergence, maximum perveance, and a minimum magnitude of the accelerator grid potential required to prevent backstreaming of beam electrons into the thruster positive high voltage surfaces. Concurrently, the efforts of this program were coordinated with those of researchers at Colorado State University who were conducting similar analytical and experimental work under NASA grant NAG3-1801.[27, 28]

Experiments

The high-power ion thruster discharge chamber was used for sub-scale ion accelerating grid tests. The thruster was installed in VF11. After each exposure to atmosphere, the cathodes were conditioned for operation. After cathode conditioning or for each test without exposure of the thruster to atmosphere, the neutralizer keeper discharge was started and then the main discharge was started. The discharges were allowed to operate for about 30 minutes prior to the application of high voltage.

All voltages were measured with digital multimeters at the vacuum tank feedthroughs. The beam voltage measurement utilized a 1000:1 high voltage probe. Precision shunts and digital multimeters were used to measure thruster currents. At some steady-state

conditions, the Faraday probe was swept across the ion beam to check for beamlet uniformity.

When the hollow cathode neutralizer was used, ions from either the neutralizer keeper discharge or from charge-exchange collisions were collected on both the accelerator grid and the domed stainless steel grid mounting plate. The resulting currents were, in some cases, comparable to the thruster generated accelerator grid currents and interfered with directly measured beam currents. Therefore, the neutralizer was not used throughout most of the test. The negative output of the high-voltage power supply was grounded and beam neutralization was achieved by secondary electron emission as the energetic ions struck the vacuum facility walls. However, this neutralization technique prevented accurate measurement of the onset of electron backstreaming. Without the hollow cathode neutralizer, the magnitude of the accelerator grid voltage could be reduced to zero with negligible impact on the indicated beam current or any other measured parameters. Reference 28 has reported that the use of hot wire filament neutralizers gave electron backstreaming results for sub-scale grids that were equivalent to those obtained with a hollow cathode neutralizer.

Results and Discussion

This section reviews the general limits of ion optics operation, using normalized per-hole parameters, and then performs detailed hole-pair designs that lead to sub-scale grid tests and a full-size grid design. Two design approaches were undertaken. The first utilized the highly successful high perveance NSTAR geometry while the other followed experimental relationships to strive for a design that allowed operation with high voltage and minimum beamlet divergence.

Limits of Ion Optics Operation

For any co-axial pair of holes in a set of 2-grid ion optics, the ability of plasma-source ions to be extracted and focused through the accelerator grid depends primarily on the ion current density along the accelerating length (or beamlet), the grid spacing, and the applied voltages. Typically, the plasma density in an ion thruster varies with radius from a peak value on-axis to a lesser value at the outer discharge chamber diameter. To separate the simultaneous contributions from the many holes in a full-size grid set with wide ranging values of current per hole, researchers have used sub-scale grids on ion sources with near constant plasma density to study the extraction of ions.[21-23,27-29] It is assumed that a grid spacing and grid total voltage exist that are sufficient to focus and accelerate the average discharge chamber ion current density.

A term called the "normalized perveance" has been used to correlate data from a variety of different ion optics geometries.[30] It can be expressed as a normalized perveance per hole (NP/H) which is defined below as

$$\frac{NP}{H} = \frac{Jh}{V_T^{3/2}}\left(\frac{le}{ds}\right)^2 \qquad (1)$$

where
Jh is the ion current per hole,
V_T is the total voltage applied to the grids,
le is the effective acceleration length for ions, and
ds is the screen grid hole diameter.

The effective acceleration length for ions is defined as

$$le = \left(lg^2 + \frac{ds^2}{4}\right)^{0.5} \qquad (2)$$

where lg is the grid-to-grid spacing. Reference 22 has shown that a theoretical limit exists for the normalized perveance per hole and it is equal to

$$\text{Maximum NP/H} = \frac{pe_0}{9}\left(\frac{2q}{m}\right)^{0.5} . \qquad (3)$$

Equation 3 defines the maximum obtainable normalized perveance per hole. The ratio q/m is the charge-to-mass ratio of the ion and ε_0 is the permittivity of free space.

For increasing values of plasma density, the plasma sheath pushes closer to the screen grid and becomes flatter such that, eventually, the trajectories of some ions diverge causing them to impinge on the accelerator grid. In this state, the ions are under-focused. This condition has been called the "impingement-limited perveance per hole."[23] The impingement-limited perveance per hole has been reported, in reference 23, to be strong functions of

three operational or geometric ratios. They are: the discharge voltage to total accelerating voltage ratio (Vd/Vt), the accelerator grid hole diameter to screen grid hole diameter ratio (da/ds), and the grid spacing to screen grid hole diameter ratio (lg/ds). The screen hole diameter, ds, has frequently been used as a geometric normalizing dimension.[21-23, 27-30]

Conversely, for decreasing values of plasma density, the plasma sheath retreats from the screen grid and becomes more concave and, in some cases, distorted[29] by neighboring holes such that the trajectories of some ions cause them to crossover and impinge on the accelerator grid. This condition has not been studied in much detail, especially when compared with the under-focused, impingement-limited perveance condition.

Between these two extreme conditions of ion impingement, the sub-scale ion beam (or single beamlet) divergence, plotted as a function of normalized perveance per hole, reaches a minimum as sketched in Figure 3.

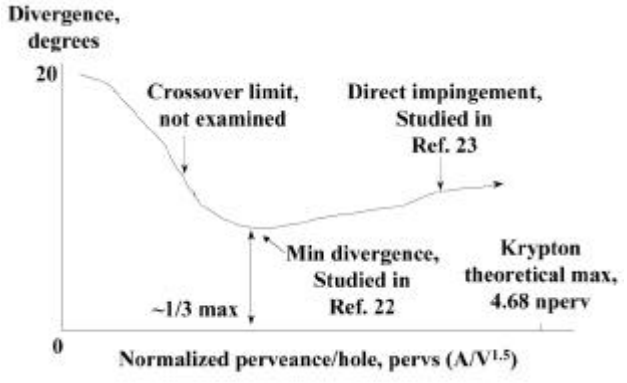

Figure 3 - Beamlet divergence as a function of normalized perveance per hole.

Figure 3 is typical of those obtained in reference 22. The minimum values of divergence were typically one-third of the maximum value. Divergence was found to be strong functions of both lg/ds and the ratio of net-to-total accelerating voltage, R. The minimum divergence decreased to lower values as lg/ds or R was increased. In that study, divergence values were presented, but the points at which accelerator impingement currents increased were not. It is believed that the accelerator-to-beam current ratio had typically varied with current per hole as sketched in Figure 4.

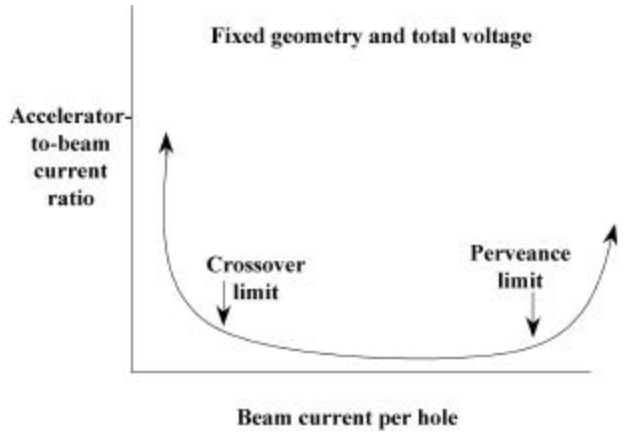

Figure 4 - Accelerator grid impingement limits.

For a fixed grid geometry and fixed grid voltages, a region of low accelerator impingement current exists, in general, where the beamlet divergence changes with decreasing or increasing beam current (or normalized perveance) per hole. Eventually, the beam ions impinge on the accelerator grid at the limits of either ion trajectory crossover (over-focused) or maximum perveance (under-focused). Obviously, the data of Figure 4 may also be plotted as a function of total accelerating voltage for a fixed beam current. In this case, the x-axis location of the perveance and crossover limits would be reversed. As mentioned earlier, the maximum perveance limit has been well documented in the past, but the crossover limit has not. The understanding of both is critical to the design of high-voltage optics for high power ion thrusters. Reference 28 presents extensive results of recent relevant experiments.

Detailed Optics Designs

First Design Approach

The first design approach to high power, high specific impulse grids resulted from the conceptual, 50-cm diameter, ion optics design, proposed in reference 20 for a 10 kW thruster. For comparison purposes only, Table 2 shows properties of the optics design proposed in reference 20 with that of the state-of-the-art (SOA), 30-cm diameter, 2.3 kW, NSTAR thruster. Both designs utilized two electrodes: a screen grid and an accelerator grid. The beam voltage was increased to satisfy the specific impulse requirement of the high power mission. At the assumed ratio of net-to-total grid voltage of 0.8, the magnitude of the negative accelerator grid voltage increased to 3250 volts from 180 volts. To obtain sufficient accelerator grid

lifetime at this high voltage (even though the average, ion-beam current density decreased by a factor of 7), a material change to carbon-carbon from molybdenum was proposed. Due to the large increase in total grid voltage, to 16,250 volts from 1280 volts, the grid-to-grid spacing increased by about a factor of 10 even with an increase in allowable electric field strength. Thus, the driver for high-power ion optics design became high voltage rather than high perveance, as it was for NSTAR.

Table 2. Ion Optics Design Comparison

Parameter	Conceptual high power design from ref. 20	NSTAR
Beam diameter, cm	50	30
Number of electrodes	2	2
Propellant	Krypton	Xenon
Beam area, cm^2	1963	642
Specific impulse, sec	14,000	3100
Beam voltage, V	13,000	1100
Net-to-total voltage, R	0.80	0.86
Beam current, A	0.77	1.76
Accelerator voltage, -V	3250	180
Grid material	Carbon-carbon	Molybdenum
Maximum allowable electric field, V/mm	2500	2050
Grid spacing, mm	6.5	0.66
Design driver	High voltage	High perveance
Thruster power, kW	10.3	2.3

To reach the new phase 2 goal of 30 kW per thruster, the beam current will increase to 2.3 A and either the beam area or the beam current density will have to triple, expanding structural or lifetime considerations.

Scaled NSTAR Design- Several studies have shown that the performance of ion optics with different designs can be specified through the use of normalized grid parameters.[22,23,30] This fact suggested that a high power optics design might be easily scaled from the highly successful NSTAR design. A scaling factor of roughly 10 was selected from the grid spacing factor shown on Table 2. This led to the grid set dimensions for the first sub-scale grid set listed in Table 1. The grid spacing and hole diameters of grid set 1 were about 10 times greater than those of the NSTAR optics. The values of sub-scale grid thickness were only about 7.5 times those of NSTAR. Optics performance is not a strong function of grid thickness.[22, 23]

Second Design Approach

Evaluations, more detailed than that of the previous section, of past and present ion optics parametric variations were conducted to obtain an "optimized" grid set design. Performance and lifetime were both considered. The design flow path started with the fact that as the beam voltage and grid spacing both increased the maximum allowable ratio of net-to-total accelerating voltage also increased. This allowed significant reductions in the total accelerating voltage and the accelerator grid voltage. The new maximum total voltage and a value of maximum electric field strength were used to obtain initial minimum values of grid spacing and screen hole diameter. An average value of beam current per hole for the high power case was estimated from prior studies of ion beam divergence. Sputtering wear calculations for the screen and accelerator grids led to minimum grid thickness values and a minimum accelerator grid hole diameter. Using a prior performance correlation, final values for the screen hole diameter and grid spacing were determined. This is only one method of reaching a hole-pair design. Depending on the assumptions, other solutions exist.

Maximum value of net-to-total accelerating voltages, R- Reference 22 showed that the ion beam divergence decreased significantly, for many variations of grid geometry, as R was increased. Reference 23 experimentally determined the maximum value of R for many cases and found that it increased with lg/ds and was nearly independent of the normalized perveance per hole. At a value of lg/ds of 1 and other anticipated grid dimensions, the maximum R was about 0.96, much higher than the value of 0.8 assumed in reference 20. This finding allowed a significant reduction of the accelerator grid voltage from 3250 volts to about 500 volts.

Minimum grid spacing, lg- Using a mission specific impulse of 14,000 seconds, krypton propellant, and a propellant utilization efficiency of 0.83, a beam voltage of about 13,000 volts was estimated. A ratio of net-to-total accelerating voltages, R, of 0.96 led to a total accelerating voltage of 13,500 volts. An assumed value of 2500 V/mm for the maximum electric field strength resulted in a grid spacing, lg, of 5.4 mm.

Minimum screen hole diameter, ds- Minimum values of ion beam divergence were obtained in reference 22 for a lg/ds of 1. Therefore, the initial minimum value of ds was also assumed to be 5.4 mm.

Average current per hole, Jha- As shown in Figure 3, the minimum ion beam divergence occurs at a value of normalized perveance per hole that is about 1/3 the maximum value, or 1.6 nanopervs for krypton. Using this as an average value for full-size grids and a total voltage of 13,500 volts gives a Jha of about 2 mA. With Jha at 2 mA and a required total beam current of 2.3 A, there might be only about 1150 grid holes. If lg and ds are 5.4 mm and the screen grid open area fraction is 0.67 (NSTAR-like), then, from a performance standpoint, the beam diameter might be only 22.4 cm, slightly less than NSTAR. But, the average beam current density would be twice that of NSTAR. Lifetime issues are addressed below.

Accelerator grid thickness, ta- Accelerator grid wear due to charge exchange phenomena primarily occurs on the downstream surface in the form of pits and grooves and as accelerator grid hole enlargement.[31,32] Both of these phenomena are determined locally and are proportional to the current density and the current per hole, respectively. To obtain an estimate of the required high power accelerator grid thickness, the following relationship of ta to grid-wear depth (due to charge-exchange ions impinging on the downstream surface), scaled to that of the NSTAR thruster, was used:

$$ta_H = \frac{jp_H}{jp_N} \cdot \frac{Q_{chexKr}}{Q_{chex,Xe}} \cdot \frac{Y_{Kr,xx}}{Y_{Xe,Mo}} \cdot \frac{T_H}{T_N} \cdot \frac{M_{xx}}{M_{Mo}} \cdot \frac{r_{Mo}}{r_{xx}} \cdot ta_N \qquad (4)$$

where
jp is the peak ion current density,
Q_{chex} is the resonant charge-exchange cross section for the propellant used,
Y is the sputter yield of the accelerator grid by propellant ions,
T is the time to wear the grid to a given depth,
M is the atomic weight of the grid material, and
r is the density of the grid material.

Subscripts H, Kr, and xx denote operational parameters of the high-power thruster case with krypton propellant and grid material (molybdenum, titanium, or stainless steel) while the subscripts N, Xe, and Mo denote operational parameters of the NSTAR thruster. It is assumed here that the ion impingement area on the accelerator grid downstream surface is independent of the accelerator grid hole diameter and that the fractional wear depth is the same in each case.

Equation 4 was used to estimate a high-power accelerator grid thickness for a 30-cm diameter NSTAR thruster using krypton propellant and molybdenum grids. Assumed values were; a jp ratio equal to the beam current ratio of 2.3 to 1.76 A, a Q_{chex} ratio of 0.57 (using the theoretical approach of reference 33 to calculate resonant charge-exchange cross sections), sputter yields from reference 34 for krypton ions on molybdenum at 500 eV of 0.87 and xenon ions on molybdenum at 180 eV of 0.27, a 10-year life requirement for the high-power thruster and the demonstrated 2-year life for NSTAR,[35] and an NSTAR ta of 0.51 mm. A high-power accelerator grid thickness of 6.1 mm was calculated. The ratio of accelerator grid thickness to screen hole diameter becomes 0.94.

Clearly, this result was beyond the typical and demonstrated range of ta/ds, which is typically 0.13 to 0.40. In addition, due to anticipated launch vibration levels, fabrication techniques will probably require NSTAR-like dished grids. That process would be complicated by the use of excessively thick grids. Therefore, methods to reduce the accelerator grid thickness were examined. From Equation 4, obvious options were to select a material with a lower sputter yield (as was done in reference 20) and/or atomic weight to density ratio or reduce the high-power current density.

Grid material- Table 3 lists several materials that were considered for high-power grids, with relative

comments. The use of carbon-carbon (C-C) material is extremely attractive because of its significantly low sputter yield, very low coefficient of thermal expansion (CTE), and low atomic mass-to-density ratio. There are ongoing efforts to develop carbon-carbon (C-C) composite ion optics at JPL[37] and GRC.[38] Part of the JPL effort is funded by a NASA Research Announcement and led by JPL to develop grids for high power, high specific impulse ion thrusters. At GRC, the goals were to greatly extend thruster lifetime and allow significant increases in beam current density. However, the fabrication costs are currently high and the performance of C-C grids has not yet matched that of metal grids.[36] Therefore, the use of C-C materials was not considered at this time for this study although they could be inserted at a later time, if necessary. Molybdenum, with its decades-long history of highly successful use on ion thrusters in ground and space tests, was considered the baseline material.

Table 3. Candidate Grid Materials

Candidate Material	Pros	Cons	Coefficient of Thermal Expansion, CTE, 10^{-6}/°C
Carbon-Carbon	Lowest sputter yield, Lightweight, Ongoing efforts at JPL & GRC	Most expensive to fabricate, Undemonstrated metal-grid-like perveance	Near 0 or negative
Molybdenum (reference material)	Long heritage, Low sputter yield	Chemical etching is moderately expensive way to fabricate holes	5
Titanium, Grade 4	Lower accelerator sputter yield, higher for screen grid	Same expense to fabricate	8.5
Titanium, Grade 2	Lower cost	Half the yield stress of grade 4	8.5
304 Stainless Steel	Inexpensive to fabricate, Easy to machine	Largest CTE, Highest sputter yield	17
465 Stainless Steel	Low cost	Magnetic	~11
Invar	Moderate CTE	CTE increases significantly for temps > 200 C, Magnetic	~1 at low temps, increasing to ~11
High-temperature Invar	Moderate CTE	Magnetic	~11
Thermo-span (Invar-like alloy)	Moderate CTE	Magnetic	~11

For molybdenum, chemical etching of the grids has been a less expensive method of fabricating many small grid holes, compared to other processes. Molybdenum also has the lowest CTE of the metal grids. Titanium, grade 4, is attractive with its 45 percent lower volumetric sputter yield in the range of interest for the accelerator grid. It has been used to fabricate grids of the NSTAR design that had nearly identical performance.[25] Fabrication costs are about the same as for molybdenum. The CTE is about 70 percent larger than for molybdenum and that with a low thermal conductivity led to a contact problem during a rapid startup of closely spaced grids. However, that problem should not occur for the high power grids with a larger spacing. A variety of steel alloys were also investigated. 304 stainless steel is the least expensive metal, but has a CTE twice that of titanium and a higher sputter yield. 465 stainless steel and the nickel alloys have lower CTE values, but are magnetic and may affect the magnetic field of the discharge chamber.

For this study, molybdenum, grade 4 titanium, and 304 stainless steel were selected for further study. The atomic mass to density ratios for these three materials are similar at about 9.4, 10.6, and 7.1, respectively. When the respective sputter yields and mass to density ratios of titanium and stainless steel were used in Equation 4, values for ta_H were only reduced to 3.8 and 5.5 mm, respectively. Therefore, it was decided to reduce the peak (and average) ion beam current density, by increasing the beam diameter, to significantly reduce the required thickness of metal accelerator grids.

Reduced current density- Because 50-cm diameter grids have been successfully fabricated in the past[39], it was decided that an increase in beam diameter to this size would conservatively reduce the maximum erosion to an acceptable level. The peak ion current density, assuming a beam current of 2.3 A and a flatness parameter of 0.5, will be about 2.3 mA/cm^2, about a third that for NSTAR. In addition, any further increases in plasma density flatness parameter will only lower the peak current density and provide more lifetime margin. An option also exists to mask the 50-cm diameter extraction area to a smaller value, if needed, to avoid current density values than are deemed too low. The expected values of ta_H, based on pit and groove erosion at the conditions above, for molybdenum, titanium, or stainless steel accelerator grids were reduced to reasonable values of 1.7, 1.1, or 1.6 mm, respectively.

Accelerator grid hole diameter, da- The other type of life limiting accelerator grid erosion is enlargement of the holes to a size that permits beam electrons to flow upstream into the discharge chamber. The volumetric sputter erosion is proportional to the product of ta and the difference between the squares of the initial and final accelerator grid hole diameters. Assuming the same fractional increase in da for the high power case as for NSTAR, Equation 5 may be used to estimate the initial accelerator hole diameter. Equation 5 is similar to Equation 4, except that a peak current per hole is used in place of a peak current density.

$$(da_H)^2 = \frac{J_{hH}}{J_{hN}} \cdot \frac{Q_{chex,Kr}}{Q_{chex,Xe}} \cdot \frac{Y_{Kr,xx}}{Y_{Mo,Xe}} \cdot \frac{T_H}{T_N} \cdot \frac{M_{xx}}{M_N} \cdot \frac{r_N}{r_{xx}} \cdot \frac{ta_N}{ta_H} \cdot (da_N)^2 \qquad (5)$$

where J_h is the peak current per hole, and da is the initial accelerator hole diameter. The subscripts are as for Equation 4. Other assumptions are that, as for NSTAR, the accelerator grid voltage will be increased over time as da increases to prevent electron backstreaming and that the charge-exchange ion production is a weak function of small changes in accelerator grid thickness and the effective accelerating lengths used here. Also, assuming J_h values of 4 and 0.2 mA per hole for the high power and NSTAR cases, respectively, and values of ta_H calculated above for each metal, the initial high-power accelerator grid hole diameters for molybdenum, titanium, and stainless steel were calculated to be 8.4, 4.5, and 4.5, respectively. At this point, based on its lower accelerator grid thickness and lower sputter yield, titanium was selected as the first choice of materials. Therefore, a conservative value of 5 mm was also chosen as the accelerator grid hole diameter.

Screen grid hole diameter, ds- High-efficiency ion thrusters use a screen to accelerator hole diameter ratio of about 0.6 to simultaneously allow high perveance ion extraction with low neutral atom losses. With high perveance expected to be less of an issue for the high power thruster and assuming a da of 5 mm, a screen hole diameter of 9 mm was selected, giving a da/ds ratio of 0.56. Maintaining an lg/ds value of 1 also led to an initial grid spacing of 9 mm. Assuming a minimum screen grid web width of 0.5 mm (67 percent more than NSTAR), the grid hole center-to-center spacing is 9.5 mm and the screen grid open area fraction is 0.81. The accelerator grid open area fraction becomes 0.25.

Screen grid thickness, ts- In addition to accelerator grid wear, another thruster life-limiting mechanism is wear of the screen grid by non-extracted discharge chamber ions. The screen grid becomes thinner as it is worn from the upstream side. This erosion, as before, is maximum on-axis at the location of peak ion current density. The maximum screen grid wear rate, w, is expressed in Equation 6 as

$$w = \frac{\left(\frac{1-f}{f}\right)\cdot Jb}{F\cdot Asg}\cdot\frac{Y_{+}+\left[0.5\cdot\left(\frac{++}{+}\right)\cdot Y_{++}\right]}{1+\left(\frac{++}{+}\right)}\cdot\frac{M}{Aq\rho} \qquad (6)$$

where
w is the maximum screen grid wear rate,
ϕ is the screen grid transparency to ions,
Jb is the ion beam current,
F is the average-to-peak beam current density ratio,
Asg is the screen grid closed area,
Y_{+} is the screen grid sputter yield from singly charged ions,
Y_{++} is the screen grid sputter yield from doubly charged ions,
(++/+) is the peak value of the doubly-to-singly-charged ion current ratio,
M is the screen grid atomic weight,
A is Avogadro's number,
q is the electronic charge, and
ρ is the screen grid density.

Equation 6 has been successfully used to compute screen grid wear for many NSTAR engineering model thrusters.[40] With the following assumptions, Equation 6 was also used to estimate krypton thruster screen grid wear over 10 years of operation at 30 kW for different grid materials. The value of ϕ was assumed to be 0.8, Jb was 2.3 A, F was 0.5, ++/+ was 0.3, and Asg was 650 cm^2.

Screen grid sputter yields were calculated from Equation 7, as suggested in reference 41 for ion energies only a few times the threshold value. It was assumed here that Equation 7 was applicable to ion energies up to 100 eV.

$$Y = K\left(E - E_{th}\right)^2 \qquad (7)$$

In Equation 7,
E_{th} is the sputtering threshold, as specified in reference 42 for a selected screen grid material,
E is the energy of the incident ion, taken as the discharge voltage for singly charged ions and twice that for doubly charged ions, and
K is a constant evaluated using tabulated sputter yield data[34] at ion energies of 100eV.

Table 4 gives values of E_{th} and K used in Equation 7 to calculate sputter yields in a krypton thruster operating with a discharge voltage of 32 volts.

Table 4. Constants Used in Equation 4

Grid material	E_{th} (ref. 42)	K (from ref. 34 data)
Molybdenum	28	1.35×10^{-5}
Titanium	17	0.44×10^{-5}
Iron (SS)	25	2.13×10^{-5}

Screen grids in early, laboratory-model NSTAR ion thrusters have been worn to half thickness (0.19 mm) without operational difficulty. Therefore, the estimated 10-year wear values were added to this minimum allowable thickness to give minimum screen grid thickness values of 1.4, 1.4, and 2.5 mm for molybdenum, titanium, and stainless steel, respectively. It was assumed that sputtered screen grid material, that deposits on discharge chamber walls and can spall and lead to electrical shorts, would be captured and retained by screen mesh covering the anode.[43]

Sub-scale Grid Tests

Scaled-NSTAR Design

Values of beam current at the perveance and crossover limits were obtained for different total accelerating voltages for grid set 1, the scaled-NSTAR design. At a net accelerating voltage of 13,000 volts, the minimum beam current, or crossover limit, was 47 mA (about 2.5 mA per hole). Extrapolating perveance limit data, taken at several lower total voltage values, to 13,500 volts yielded an expected maximum 14 mA per hole.

Figure 5 presents Faraday beam probe traces, as a function of probe distance downstream of the accelerator grid. The probe travel was horizontal, across 5 holes of the grid diameter. As assumed, the discharge chamber plasma was quite uniform. The beam spread was estimated to be about 12 degrees, comparable to that predicted by the OPT code. For this geometry, reference 23 predicted a reduced ratio of net-to-total accelerating voltages that would lead to higher magnitude accelerator grid voltages. Indeed, the major drawback of this design was that at beam current per-hole values of interest the negative accelerator grid voltage required to prevent electron backstreaming from the hollow cathode neutralizer was in excess of 1000 volts. Thus, the investigation of this design was discontinued.

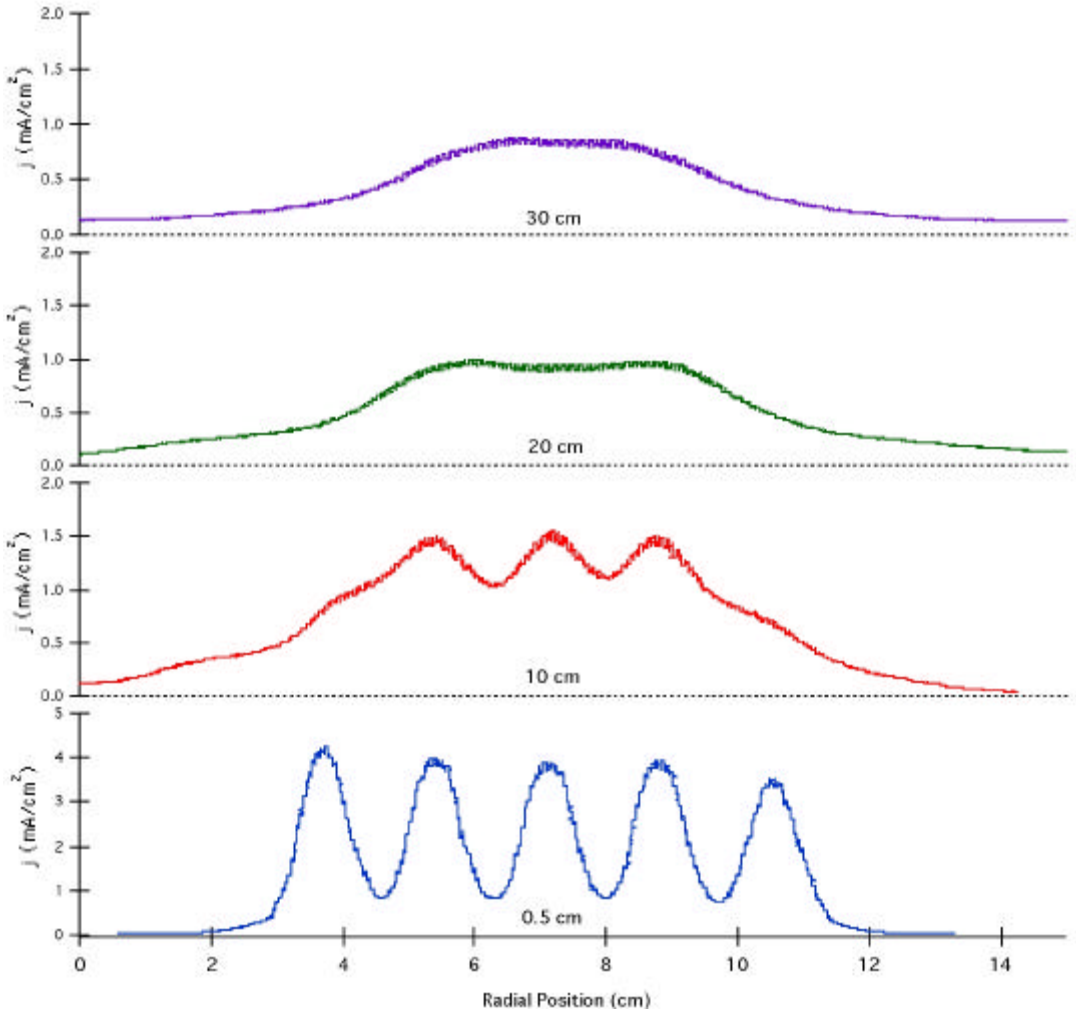

Figure 5 - Faraday probe traces as functions of distance downstream of accelerator grid (grid set 1 operated at 12,000 volts, net voltage and 70 mA beam current).

Optimized Grid Design

Grid Set 2, da = 4 mm- Use of Equation 5 gave a value of 4.5 mm for da. While 5 mm was selected, a da of 4 was experimentally evaluated here and in reference 28. Values of total accelerating voltage at the crossover and perveance limits were obtained for different values of beam current for grid sets 2 and 3. With grid set 2, propellant isolator problems prevented data from being obtained at beam voltages greater than 10,000 volts. It was found for both grid sets that the ratio of beam current at the perveance limit divided by the three-halves power of the total voltage increased nearly linearly with increasing total accelerating voltage. The ratio for the crossover limit current was essentially independent of the total accelerating voltage. When these functions were extrapolated to the desired 13,500-volt point for grid set 2, crossover and perveance current limit values of about 1.2 and 3.8 mA per hole, respectively, were obtained for a cold grid spacing of 9 mm. Comparing these results with those interpolated from data presented in reference 28, the crossover limit current per hole found herein was about 25 percent lower than that expected from reference 28. The maximum perveance limit current was about 80 percent greater than that expected from reference 28.

It is postulated that two separate effects contributed to the increase in the ratio of perveance limit current to total voltage, mentioned above, with total voltage (or beam current). First, beamlet shape distortion decreases with increasing values of current per hole.[28,29] Secondly, the increased discharge power, required to produce the higher values of beam currents at the maximum perveance current limits, may have led to smaller values of hot grid spacing for the results presented herein. This is because the sub-scale grid plates were mounted to non-perforated domed stainless steel disks that have a

greater CTE than titanium grids or molybdenum NSTAR grids. The non-perforated screen grid mounting disk would also receive most of the heating, shield the accelerator-grid mounting disk, and thus, move the screen grid closer to the accelerator grid. A spacing decrease here of only a few millimeters would lead to higher perveance limit currents that would be in agreement with those of reference 28.

As expected from reference 23, the maximum ratio of net-to-total accelerating voltages were greater than 0.96. This allowed the magnitude of the accelerator grid voltage to remain less than 500 volts for all testing of grid sets 2 and 3, even when the hollow cathode neutralizer was employed.

Grid set 3, da = 5 mm- A crossover limit beam current value of 0.63 mA per hole was directly measured at 13,100 volts for grid set 3. This is much lower than that expected when compared to data from grid set 2 or reference 28. The reason for this is unknown. Perveance limit current data were taken and extrapolated, as above, to yield a 13,500 volt current limit of 4.1 mA per hole. This value is about 60 percent greater than that interpolated from reference 28 and, as expected, slightly greater than that for grid set 2. Again, the hot grid spacing may have been less than the cold value. The wide range of allowable beam currents between the crossover limit and perveance limit for this geometry fortified its selection for full-size optics.

Final Electrode Design

Table 5 lists the nominal parameters selected for electrodes that are currently being fabricated for the 30 kW krypton ion thruster. The material is titanium, grade 4. The screen and accelerator grid hole diameters are 9 and 5 mm, respectively. Two values of grid thickness were chosen for each grid to evaluate their effects on both fabrication techniques and performance.

For the grid geometry shown in Table 5 and a beam current of 2.3 A, an average current per hole of 0.92 mA is obtained. Assuming a beam flatness of 0.5, the peak current per hole is about 1.8 mA. As a result of lowering the peak beam current density to obtain a reasonable accelerator grid thickness, the average value of the current per hole was also lowered. This means that the average normalized perveance per hole is about 0.73 nanopervs: a value less than the desired value of 1.6 nanopervs that gives the minimum beamlet divergence. It is expected that the focusing properties of full-size grids will be adjusted, as necessary, with changes in the grid spacing, flatness of the discharge chamber plasma density, and grid extraction area.

Table 5. High Power Optics Design

Material	Titanium
Beam diameter, cm	50
Number of holes	2500
Hole center-to-center spacing, mm	9.5
Screen hole diameter, mm	9.0
Screen grid thickness, mm	1.0 and 1.5
Screen grid open area fraction	0.81
Accelerator grid hole diameter, mm	5
Accelerator grid thickness, mm	1.5 and 2.0
Accelerator grid open area fraction	0.25
Initial grid spacing, mm	9
Initial electric field, V/mm	1500

Figure 6 shows the OPT code output for the finalized grid design with inputs from Table 5.

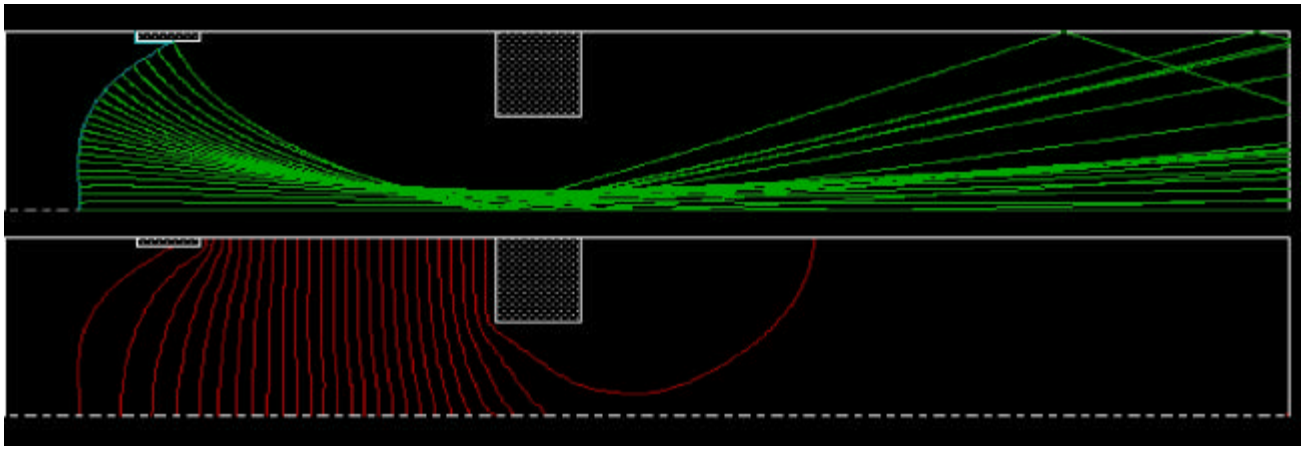

Figure 6. OPT code results for finalized grid design.

The upper part of the figure shows ion trajectories from half of a hole with the average perveance of 0.73 nanopervs. While there is some beam spread at this low value of perveance per hole, there is no direct impingement on the accelerator grid. This is consistent with experimental data presented above. The lower portion shows equipotential contours, in 500-volt increments, when the screen grid is at 13,000 volts and the accelerator grid is at -500 volts.

Conclusions

The second phase of a program to develop a high power, high specific impulse krypton ion engine to support energetic space missions has begun. A high-voltage ion optics design was chosen, for an assumed mission, as a result of detailed performance and lifetime analyses and inexpensive sub-scale grid fabrication and operation. Full-size 50-cm diameter, grade 4, titanium ion optics with values of spacing, thickness, and hole diameters, significantly greater than those of NSTAR are being fabricated.

Three sub-scale two-grid ion optics geometries were tested at voltages up to 13,000 volts. They all yielded values of krypton beam current that, when scaled to full-size 50-cm diameter, could produce ion beams with powers between 20 and 30 kW at values of specific impulse in excess of 14,000 seconds.

It was found for all three sub-scale grid sets that, for a selected set of beam and accelerator grid voltages, there were lower and upper limits of ion current per grid hole between which operation resulted in focused ion beams. Thus, the uniformity of the discharge chamber will be important toward maintaining operation within these limits. To avoid electrical breakdown between the grids, the grid spacing was increased significantly. For the sub-scale grid sets with large grid spacing, operation with an accelerator grid voltage magnitude of less than 500 volts was demonstrated. Based on this voltage magnitude, metal grids were chosen for this program to avoid fabrication risks and costs of large area carbon-carbon based ion optics which were anticipated in this program's first phase.

References

1. http://umbra.nascom.nasa.gov/SEC/secr/missions/ISP.html
2. Johnson, L. and Leifer, S., "Propulsion Options for Interstellar Exploration," AIAA Paper 2000-3334, July 2000.
3. http://spacescience.nasa.gov/ao/01-oss-01/index.html
4. http://www.jpl.nasa.gov/ice_fire
5. Sovey, J.S., et al., "Development of an Ion Thruster and Power Processor for New Millennium's Deep Space 1 Mission," AIAA Paper 97-2778, July 1997.
6. http://nmp.jpl.nasa.gov/ds1/
7. Reader, P.D., "Experimental Performance of a 50-Centimeter Diameter Electron-Bombardment Ion Rocket," AIAA Paper 64-689, 1964.
8. Nakanishi, S. and Pawlik, E.V., "Experimental Investigation of a 1.5-m-diam Kaufman Rocket," Journal of Spacecraft and Rockets, Vol.5, No. 7, July 1968, pp. 801-807.
9. Staff of Lewis Research Center, Cleveland, Ohio, "A Case History of Technology Transfer," NASA TM-82618, August 1981.
10. Cybulski, R.C., et al., "Results from SERT I Ion Rocket Flight Test," NASA TN D-2718, March 1965.
11. Kerslake, W.R. and Ignaczak, L.R., "Development and Flight History of the SERT II Spacecraft," AIAA Paper 92-3516, July 1992.
12. Duxbury, J.H., "A Solar-Electric Spacecraft for the Encke Slow Flyby Mission," AIAA Paper 73-1126, Nov. 1973.
13. Anon., "30-Centimeter Ion Thrust Subsystem Design Manual," NASA TM-79191, June 1979.
14. Power, J.L., "Planned Flight Test of a Mercury Ion Auxiliary Propulsion System-Objectives, System Descriptions, and Mission Operations," AIAA Paper 78-647, April 1978.
15. Rawlin, V.K., "Operation of the J-Series Thruster Using Inert Gas," AIAA Paper 82-1929, Nov. 1982.

16. Poeschel, R.L., "Development of Advanced Inert-Gas Ion Thrusters," NASA CR-168206, Hughes Research Laboratories, June 1983.

17. Sovey, J.S., Rawlin, V.K., and Patterson, M.J., " Ion Propulsion Development Projects U.S.: Space Electric Rocket Test I to Deep Space 1," *Journal of Propulsion and Power, Vol. 17, No. 3, 517-526*, May-June 2001.

18. Beattie, J.R., Williams, J.D., and Robson, R.R., "Flight Qualification of an 18-mN Xenon Ion Thruster," IEPC Paper 93-106, Sept. 1993.

19. "XIPS: The Latest Thrust in Propulsion Technology," URL: http://www.hsc.com/factsheets/xips/xips.html

20. Patterson, M.J., Roman, R.F., and Foster, J.E., "Ion Engine Development for Interstellar Precursor Missions," AIAA Paper 2000-3811, July 2000.

21. Aston, G. "The Ion-Optics of a Two-Grid Electric Bombardment Thruster," NASA CR-135034, Colorado State University, May 1976.

22. Aston, G., Kaufman, H.R., and Wilbur, P.J., "Ion Beam Divergence Characteristics of Two-Grid Accelerator Systems," *AIAA Journal, Vol.16, No. 5, 516-524*, May 1978.

23. Rovang, D.C., "Ion Extraction Capabilities of Two-Grid Accelerator Systems," NASA CR-174621, Colorado State University, Feb. 1984.

24. Nakayama, Y. and Wilbur, P.J., "Numerical Simulation of Ion Beam Optics for Many-grid Systems," AIAA Paper 2001-3782, July 2001.

25. Soulas, G.C., Foster, J.E., and Patterson, M.J., "Performance of Titanium Optics on a NASA 30 cm Ion Thruster," AIAA Paper 2000-3814, July 2000.

26. Piñero, L.R., Patterson, M.J., and Satterwhite, V.E., "Power Console Development for NASA's Electric Propulsion Outreach Program," IEPC Paper 93-250, Sept. 1993.

27. Nakayama, Y. and Wilbur, P.J., "Numerical Simulation of High Specific Impulse Ion Thruster Optics," IEPC Paper 01-099, Oct. 2001.

28. Wilbur, P.J., et al., "A Study of High Specific Impulse Ion Thruster Optics," IEPC Paper 01-098, Oct. 2001.

29. Hayakawa, Y. and Kitamura, S., "Ion Beamlet Divergence Characteristics of Two-Grid Multiple-Hole Ion Accelerator Systems," AIAA Paper 97-3195.

30. Kaufman, H.R., "Technology of Electron-Bombardment Ion Thrusters," *Advances in Electronics and Electron Physics, Vol. 36, 265-373*, L. Marton, ed., Academic Press, Inc., New York, 1974.

31. Rawlin, V.K., "Erosion Characteristics of Two-Grid ion Accelerating Systems," IEPC Paper 93-175, Sept. 1993.

32. Polk, J.E., et al., "An Overview of the Results from an 8200 Hour Wear Test of the NSTAR Ion Thruster," AIAA Paper 99-2446, June 1999.

33. Rapp, D. and Francis, W.E., *Journal of Chem. Phys., **37**, 2631-2645, 1962.*

34. Rosenberg, D. and Wehner, G.K., "Sputtering Yields for Low Energy He^+-, Kr^+-, and Xe^+- Ion Bombardment," *Journal of Applied Physics, Vol. 33, No. 5, 1842-1845*, May 1962.

35. Anderson, J.R., et al., "Long Duration Ground Testing of the Deep Space 1 Flight Spare Ion Thruster-the First 15,600 Hours," IEPC Paper 01-076, Oct. 2001.

36. Mueller, J., Brophy, J.R., and Brown, D.K., "Design, Fabrication, and Testing of 30-cm Dia. Dished Carbon-Carbon Ion Engine Grids," AIAA Paper 96-3204, July 1996.

37. Shotwell, R., "Carbon-Carbon Grid Development for Advanced Ion Propulsion Systems," IEPC Paper 01-093, Oct. 2001.

38. Haag, T., et al., "Carbon-based Ion Optics Development at NASA GRC," IEPC Paper 01-094, Oct. 2001.

39. Rawlin, V.K. and Millis, M.G., "Ion Optics for High Power 50-cm-diam Ion Thrusters," AIAA Paper 89-2717, July 1989.

40. Brophy, J.R., Polk, J.E., and Rawlin, V.K., "Ion Engine Service Life Validation by Analysis and Testing," AIAA Paper 96-2715, July 1996.

41. Wilhelm, H.E., "Theoretical Investigation of Plasma Processes in the Ion Bombardment Thruster," NASA CR-13471, 1971.

42. Stuart, R.V. and Wehner, G.K., "Sputtering Yields at Very Low Bombarding Ion Energies," *Journal of Applied Physics, Vol. 33, No. 7, 2345-2352*, July 1962.

43. Sovey, J.S., Dever, J.A., and Power, J.L., "Retention of Sputtered Molybdenum on Ion Engine Discharge Chamber Surfaces," IEPC Paper 01-086, Oct. 2001.